Cathepsin S regulates renal fibrosis in mouse models of mild and severe hydronephrosis

XIAOBING YAO[1], FAN CHENG[1], WEIMING YU[1], TING RAO[1], WEI LI[2], SHENG ZHAO[1], XIANGJUN ZHOU[1] and JINZHUO NING[1]

Departments of [1]Urology and [2]Anesthesiology, Renmin Hospital of Wuhan University, Wuhan, Hubei 430060, P.R. China

Received August 17, 2018; Accepted May 2, 2019

DOI: 10.3892/mmr.2019.10230

Abstract. As a member of the cysteine protease family, cathepsin S (CTSS) serves an important role in diseases such as cancer, arthritis and atherosclerosis. Nevertheless, its role in renal fibrosis is unknown. In the present study, the effects of CTSS on renal fibrosis in mild (group M) and severe (group S) hydronephrosis were studied by reverse transcription-quantitative PCR (RT-qPCR), western blot analysis (WB), Masson's trichrome staining and immunohistochemical staining in mouse models. The effects of CTSS on extracellular matrix (ECM) deposition and epithelial-mesenchymal transition (EMT) and the potential mechanisms were further studied by RT-qPCR and WB in transforming growth factor (TGF-β1)-stimulated TCMK-1 cells. Compared with group N (no hydronephrosis), the expression levels of CTSS in the M and S groups were significantly higher, and a significant increase in ECM deposition was observed in the S group. In addition, compared with group N, the expression levels of TGF-β1, α-smooth muscle actin (α-SMA), SMAD2, SMAD3, phosphorylated (p)SMAD2 and pSMAD3 in groups M and S were significantly higher, whereas the expression of E-cadherin was significantly lower. Inhibition of CTSS expression increased the expression levels of TGF-β1, α-SMA, fibronectin, collagen-I, SMAD2, SMAD3, pSMAD2 and pSMAD3, whereas E-cadherin expression decreased. A significant increase in CTSS was observed in the TGF-β1-stimulated TCMK-1 cell line. ECM deposition and EMT were also intensified. The opposite outcomes occurred after intervention with small interfering RNA targeting CTSS. In conclusion, CTSS affected EMT and the deposition of ECM. CTSS may mediate the regulation of fibrosis by the TGF-β/SMAD signaling pathway. CTSS may serve an important role in the treatment of renal fibrosis.

Correspondence to: Professor Fan Cheng, Department of Urology, Renmin Hospital of Wuhan University, 238 Jiefang Road, Wuhan, Hubei 430060, P.R. China
E-mail: urology1969@aliyun.com

Key words: cathepsin S, hydronephrosis, renal fibrosis, transforming growth factor-β1, SMAD

Introduction

Renal fibrosis is a long-term manifestation of tissue damage (1,2). During its progression, as normal renal tissues and structures are gradually replaced by extracellular matrix (ECM), renal function declines, eventually leading to end-stage renal failure (3,4). Although cathepsin S (CTSS) generally degrades unwanted proteins inside cells, cysteine cathepsins also bind to cell surface receptors on the plasma membrane in the pericellular environment, are involved in soluble enzyme activity and may even be detected in secretory vesicles, cytosol, mitochondria and within the nuclei of eukaryotic cells (5-7). CTSS participates not only in the regulation of hepatic fibrosis but also in ventricular remodeling after myocardial infarction (8). A number of reports have indicated that CTSS serves an important role in the pathogenesis of fibrotic diseases such as airway fibrosis, atherosclerosis and Sjögren's syndrome (9-12). Therefore, it is necessary to clarify whether CTSS is involved in renal fibrosis and to explore its mechanisms. TGF-β is a secreted protein, and many related studies have confirmed the important role of TGF-β in the process of fibrosis, which regulates EMT and promotes the proliferation and activation of interstitial fibroblasts. Whether the effect of CTSS on renal fibrosis is related to TGF-β was also studied.

In clinical practice, patients with urinary stones, especially upper urinary tract stones, often have varying degrees of accompanying hydronephrosis. Our previous studies demonstrated that hydronephrosis increased damage to the kidneys (13,14). However, hydronephrosis is not only associated with injury; there are also reports of hydronephrosis with fibrosis (15,16). In addition, the severity of hydronephrosis may be an important factor in the treatment of upper urinary tract stones; treatment options often depend on the degree of hydronephrosis. Therefore, whether different degrees of hydronephrosis have different effects on renal fibrosis is another issue that needs to be addressed.

In the present study, the relationship between hydronephrosis and renal fibrosis was demonstrated. The role of CTSS in the pathogenesis of renal fibrosis was also studied in a mouse model of mild and severe hydronephrosis. The results indicated that CTSS may be an important influencing factor in the process of renal fibrosis.

Materials and methods

Animals and groups. A total of 36 Male C57BL/6 mice (20-25 g, 6 weeks old) were purchased from the Center of Experimental Animals of Wuhan University (Hubei, China). The mice were caged in a standard temperature-controlled room with alternating 12-h light/dark cycles, with free access to water and a standard laboratory diet. The environmental temperature was maintained at 20-25˚C and the humidity was maintained at 50-52%. The study received approval from the Wuhan University Committee on Ethics for Animal Experiments.

The animals were randomly divided into two groups, the control group and the inhibitor group. Each group was divided into three subgroups (n=6 mice/group): The no hydronephrosis (N) groups (N, 'no inhibitor'; Ni, 'inhibitor'); the mild hydronephrosis (M) groups (M, 'no inhibitor'; Mi, 'inhibitor'); and the severe hydronephrosis (S) groups (S, 'no inhibitor'; Si, 'inhibitor').

Surgical manipulation. Mice were anesthetized with 0.3% pentobarbital sodium [30 mg/kg; intraperitoneal (i.p.) injection]. The mice were supine on a temperature-controlled operating table. A 1.5-3 cm incision was made in the left lower abdomen, exposing the left ureter. A polyethylene catheter (~2 cm) was cut open lengthwise and placed in the ureter The upper and lower ends of the polyethylene catheter were ligated, and the abdominal cavity was closed and sterilized. In the N groups, the abdominal cavity was opened without ligation of the ureter. Penicillin was injected i.p. every day after surgery to prevent infection.

B-ultrasound examination was performed on day 3 post-surgery in the M groups and on day 7 in the S groups to determine the formation of hydronephrosis. Various degrees of renal hydronephrosis were observed. In the N groups, no separation of the collection system was observed. In the M groups, separation of the collection system and a small number of liquid dark areas were observed; in the S group, the collection system was significantly separated, with renal parenchymal thinning and fluid dark areas occupying most of the kidney. B-ultrasound was used to examine the degree of renal pelvis dilation and the thickness of the renal parenchyma to determine whether the mild and severe hydronephrosis model was successfully constructed. In the 'inhibitor' groups, all mice were treated identically, and the CTSS inhibitor LY3000328 (30 mg/kg; Absin, abs811344; http://www.univ-bio.com/goods-5951366-abs811344-5mg-Z-FL-COCHO.html) was administered orally twice per day from day 1. The Ni group was given the solvent for LY3000328 (1% Sodium Carboxymethyl Cellulose).

The mice were sacrificed after 48 h, and the kidneys were harvested. Kidney tissue was randomly divided into two parts; one part fixed in 4% paraformaldehyde for paraffin embedding and the other part preserved in liquid nitrogen for western blotting and other tests.

Masson's trichrome staining. The Masson staining kit (Servicebio Inc., G1006) was used in accordance with the manufacturer's protocol. The 4-μm sections were warmed at 60˚C for 45 min, and placed in xylene I 20 min, xylene II 20 min, absolute ethanol I 5 min, absolute ethanol II 5 min, 75% alcohol 5 min and a tap water wash x2. For sodium dichromate staining the section was soaked in 3% potassium dichromate at room temperature overnight then washed with tap water three times before staining in iron hematoxylin for 3 min followed by washing with tap water, differentiation with acid alcohol and rinsing with tap water four times. Then the section were stained with Lichun red acid magenta for 5-10 min followed by rinsing with tap water. Foe the 5, phosphomolybdic acid step, the sections were placed in phosphomolybdic acid aqueous solution for 1-3 min. For the aniline blue staining the sections were directly into the aniline blue dye solution for 3-6 min. The sections were differentiated with 1% glacial acetic acid and dehydrated with two changes of absolute ethanol before a third immersion in absolute ethanol for 5 min followed by clearing in xylene for 5 min and mounting in neutral gum seal.

Immunohistochemical staining. The oven was set to 60˚C, and the sections baked for 45 min; the dewaxed sections were reacted with xylene at room temperature for 10 min 3 times; then the sections were placed in gradient concentrations of alcohol (anhydrous, 95, 85 and 75%) for 5, 2 min (twice), 2 and 2 min respectively. The residual ethanol was washed off with tap water and the section soaked in distilled water for 2 min twice. PBS solution (Hyclone; GE Healthcare Life Sciences, SH30256.01) was added to the section for 5 min and the section then immersed in an antigen retrieval solution (Servicebio Inc., G1201), and the antigen was retrieved by microwave (low power 5 min, medium power 10 min). Endogenous peroxidase was removed using 3% hydrogen peroxide and the following primary antibodies were added: α-Smooth muscle actin [α-SMA; 1:200; cat. no. 19245T; Cell Signaling Technology, Inc. (CST)], E-cadherin (1:400; cat. no. 3195T; CST), transforming growth factor β1 (TGF-β1; 1:100; cat. no. ab92486; Abcam), CTSS (1:50; cat. no. Sc271619; Santa Cruz Biotechnology, Inc.), collagen-I (1:100; cat. no. ab34710; Abcam) and fibronectin (FN; 1:200; cat. no. ab2413; Abcam). Sections were incubated at 37˚C for 2 h and maintained overnight at 4˚C.

Biotin-labeled secondary antibody was added dropwise (secondary antibody was derived from immunohistochemistry kit, OriGene Technologies, Inc., SPN-9001, 9002), diluted 1:300 in 1% BSA-PBS, incubated at 37˚C for 30 min and then rinsed in PBS for 3 min 3 times. Horseradish enzyme labeled streptavidin was added dropwise and then section rinsed in PBS for 3 min 3 times. Color development was performed with a developer (DAB; OriGene Technologies, Inc., ZLI-9017). The reaction was observed under a routine brightfield microscope (magnification, x400; BX51; Olympus Corporation), followed by washing with water to stop the reaction.

Ten fields of view were randomly selected for each slice and analyzed with ImagePro-Plus 6.0 (Media Cybernetics, Inc.). Two parameters, positive area (Area) and integrated optical density (IOD), were measured. The mean optical density (MOD=IOD/Area) was calculated to measure the expression of indicators.

Western blotting. Frozen kidney tissue was homogenized on ice, and RIPA lysate containing PMSF was added for 30 min

(1 ml RIPA lysate to 100 mg of tissue). The mixture was centrifuged at 12,000 x g and 4˚C for 15 min), the supernatants were removed, loading buffer was added and boiled for 8 min. Following cooling, proteins were stored at -20˚C. Protein concentrations were measured using the bicinchoninic acid assay. Proteins (50 μg) were separated by 12% SDS-PAGE, transferred onto PVDF membranes and blocked with 5% skimmed milk at room temperature for 2 h. The PVDF membranes were incubated with primary antibodies overnight at 4˚C. The PVDF membranes were subsequently rinsed with -Tris-HCl buffer containing Tween-20 (1 ml Tween-20 to 1000 ml Tris-HCl buffer) and the reaction with the secondary antibody was carried out for 1 h at room temperature. The Odyssey infrared imaging system (LI-COR Biosciences) was used to analyze the expression levels of the target protein and the relative band intensity was quantified using Quantity One 4.6.2 software (Bio-Rad Laboratories, Inc.). GAPDH was used as an internal reference. The following antibodies were used in this process: CTSS (1:100; cat. no. sc271619; Santa Cruz Biotechnology, Inc.), α-SMA (1:1,000; cat. no. 19245T; CST), E-cadherin (1:1,000; cat. no. 3195T; CST), TGF-β1 (1:500; cat. no. ab92486; Abcam), FN (1:200; cat. no. ab2413; Abcam), collagen-I (1:1,000; cat. no. ab34710; Abcam), SMAD2 (1:1,000; cat. no. 5339S; CST), SMAD3 (1:1,000; cat. no. 9513S; CST), phosphorylated (p)-SMAD2 (1:1,000; cat. no. 18338S; CST), p-Smad3 (1:1,000; cat. no. 9520S; CST), GAPDH (1:1,000; cat. no. 5174S; CST), anti-mouse secondary antibody (1:15,000; cat. no. 5257P, CST) and anti-rabbit secondary antibody (1:30,000; cat. no. 5151S; CST).

Reverse transcription-quantitative PCR. Total RNA from kidney tissue (1 g) was extracted using the TRIzol kit (cat. no. 155960026; Invitrogen; Thermo Fisher Scientific, Inc.). Reverse transcription was performed with RevertAid Reverse Transcriptase (cat. no. EP0442; Fermentas; Thermo Fisher Scientific, Inc.), dNTP (cat. no. R0191; Fermentas; Thermo Fisher Scientific, Inc.) and RiboLock RNase Inhibitor (cat. no. E00381; Fermentas; Thermo Fisher Scientific, Inc.). qPCR was performed using an ABI StepOnePlus Real-Time PCR instrument (Applied Biosystems; Thermo Fisher Scientific, Inc.). The following reagents were used: KAPA SYBR FAST qPCR kit Master Mix (2X) and ABI Prism (Kapa Biosystems, Inc., KR0390). The thermocycling consisted of an initial denaturation for 3 min at 95˚C, followed by 40 cycles of 3 sec at 95˚C and 30 sec at 60˚C. The results were analyzed using the $2^{-\Delta\Delta Cq}$ method (17). The sequences of primers for kidney specimens were as follows: CTSS, forward 5'-ATAAGATGGCTGTTTTGGATG-3', reverse 5'-TTCTTTTCCCAGATGAGACGC-3'; α-SMA, forward 5'-CCACCGCAAATGCTTCTAAGT-3', reverse 5'-GGCAGGAATGATTTGGAAAGG-3'; E-cadherin, forward 5'-AGCCAGACACATTCATGGAAC-3', reverse 5'-TCGTTATCCGAGATTGAGA-3'; FN, forward 5'-AGGCTGGATGATGGTGGACT-3', reverse 5'-CGGCTGAAGCACTTTGTAGAG-3'; collagen-I, forward 5'-CAAGAAGACATCCCTGAAGTC-3', reverse 5'-ACAGTCCAGTTCTTCATTGC-3' (Invitrogen; Thermo Fisher Scientific, Inc.). The transcript levels of the target genes were normalized to the β-actin gene. The sequences of the β-actin primers were: β-actin, forward 5'-CTGAGAGGGAAATCGTGCGT-3', reverse 5'-CCACAGGATTCCATACCCAAGA-3' (Invitrogen; Thermo Fisher Scientific, Inc.).

Cell culture and treatment. The tubular epithelial cell line TCMK-1 (cat. no. CCL-139; American Type Culture Collection) was cultured in DMEM containing 10% FBS (Gibco; Thermo Fisher Scientific, Inc.) and 1% penicillin-streptomycin and incubated at 37˚C in 5% CO_2. The siRNA and RNAi sequences targeting the mouse CTSS gene were designed and synthesized by Guangzhou RiboBio Co., Ltd. The siRNA sequence was as follows: 5'-CTACAAAGCCACGGATGAA-3'. 5'-TTCGCGACAAAACAGACGA-3' was used as a negative control. TGF-β1 (Bio-Techne, 7666-MB) was added 12 h after siRNA treatment.

Statistical analysis. Data are expressed as the mean ± SD. Statistical significance was assessed by ANOVA with subsequent Student-Newman-Keuls test using SPSS 15.0 software (SPSS, Inc.). $P<0.05$ was considered to indicate a statistically significant difference.

Results

CTSS expression in kidneys with various degrees of hydronephrosis and TGF-β1 increases the expression of CTSS in TCMK-1 cells. siRNA-CTSS inhibits the expression of CTSS in TCMK-1 cells. The expression of CTSS in the hydronephrotic kidney was examined. Within the N, M and S groups, the expression of CTSS in the control group was significantly higher compared with the inhibitor group (Fig. 1A-E). The expression of CTSS in the M and S groups was significantly higher compared with the N group (Fig. 1B). Changes in CTSS expression in TCMK-1 cells were measured following 24-h incubation with 1, 5 or 10 ng/ml TGF-β1 or no TGF-β1 (control). TGF-β1 increased the expression of CTSS in TCMK-1 cells at an optimal TGF-β1 concentration of 10 ng/ml (Fig. 1F-H). WB and PCR confirmed that the siRNA-CTSS constructed for the present study can effectively inhibit the expression of CTSS in TCMK-1 cells (Fig. 1I-K).

Fibrosis with hydronephrosis and TCMK-1 cell fibrosis induced by TGF-β stimulation are associated with enhancement of ECM accumulation and epithelial-mesenchymal transition (EMT), the TGF-β/Smad signaling pathway has also been affected. ECM deposition in hydronephrotic kidneys was greater compared with normal kidneys. Significant increases in the expression of collagen-I, FN, SMAD2 and SMAD3 were observed in the S group compared with the N group (Figs. 2A-I and 3A, C and D). In addition, the expression levels of TGF-β1, α-SMA, p-SMAD2 and pSMAD3 were significantly higher in the M and S groups, whereas the levels of E-cadherin were lower compared with the N group (Figs. 3A, E-H and 4A-I). Masson's trichrome staining demonstrated increased fibrosis in the hydronephrotic kidneys compared with normal kidneys (Fig. 5A).

In TGF-β1-stimulated TCMK-1 cell lines, western blotting and RT-qPCR assays revealed significant increases in α-SMA, COL-1, FN, SMAD2, SMAD3, pSMAD2 and pSMAD3 expression levels and a decrease in E-cadherin compared with non-stimulated cells (Figs. 2J-N, 3B, I-L and 4J-N).

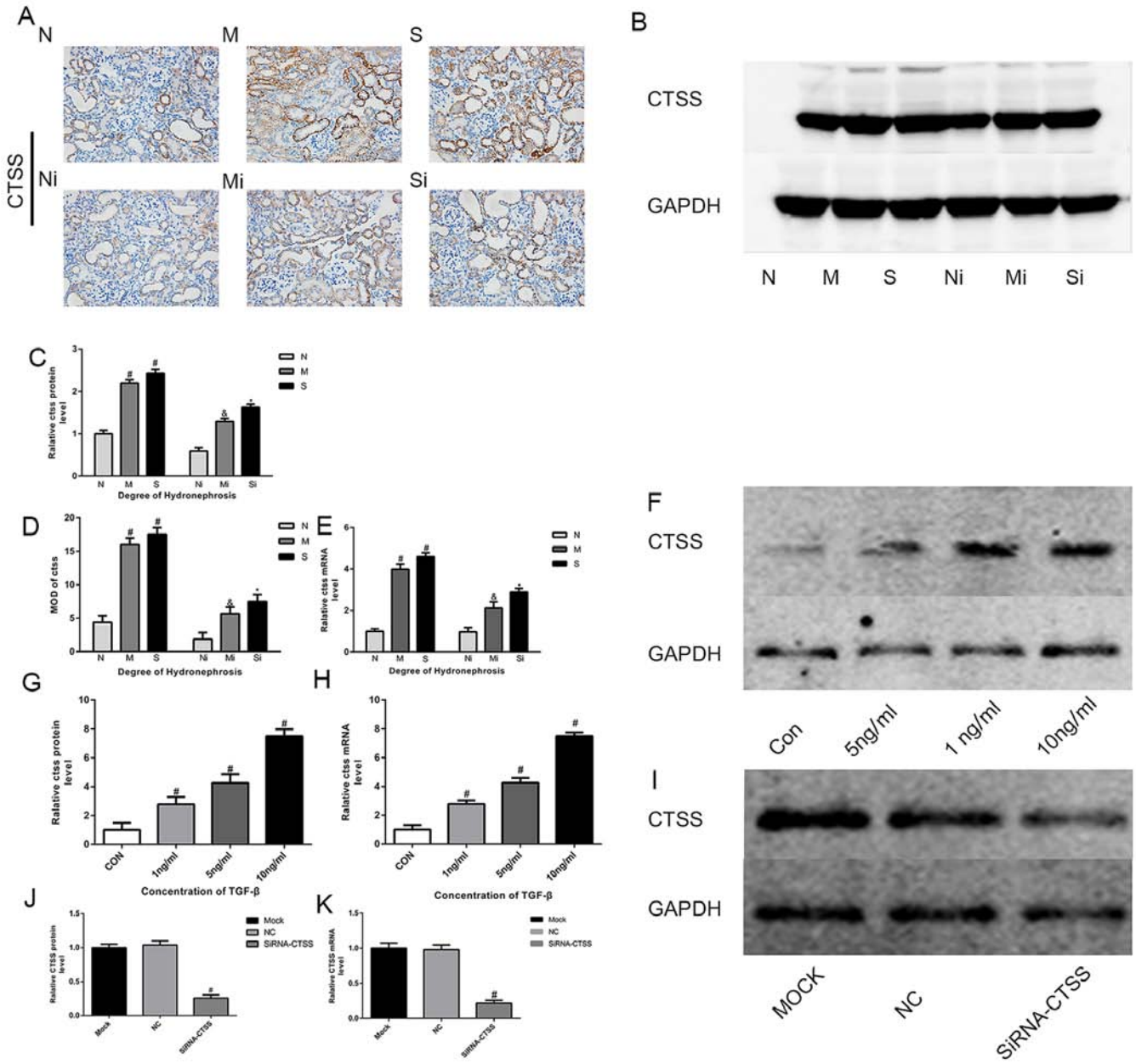

Figure 1. CTSS inhibitor treatment decreased the expression of CTSS in mouse kidneys, whereas TGF-β1 treatment increased the expression of CTSS in TCMK-1 cells. (A and D) CTSS measured by immunohistochemistry (magnification, x400) in mice treated with LY3000328 or not; (B and C) CTSS measured by WB in mice treated with LY3000328 or not; (E) CTSS measured by qPCR in mice treated with LY3000328 or not; (F and G) CTSS measured by WB in TCMK-1 cells stimulated by different concentrations of TGF-β1; (H) CTSS measured by qPCR in TCMK-1 cells stimulated by different concentrations of TGF-β1; (I and J) CTSS measured by WB in TCMK-1 cells treated by siRNA-CTSS; (K) CTSS measured by qPCR in TCMK-1 cells treated by siRNA-CTSS. The data are shown as the mean ± standard deviation; $^{\#}$P<0.05 vs. the N group, $^{\&}$P<0.05 vs. the M group, *P<0.05 vs. the S group. Grouping: The N groups (N-no inhibitors, Ni-inhibitors), no hydronephrosis; the M groups (M-no inhibitors, Mi-inhibitors), mild hydronephrosis; and the S groups (S-no inhibitors, Si-inhibitors), severe hydronephrosis. CTSS, cathepsin S; TGF, transforming growth factor; WB, western blotting; qPCR, quantitative PCR.

Inhibition of CTSS expression affects renal fibrosis. Following CTSS inhibition, the expression levels of COL-1, FN, α-SMA, pSMAD2 and pSMAD3 were significantly higher, whereas the expression levels of E-cadherin were lower in the 'inhibitor' groups compared with the 'no inhibitor' groups (Figs. 2A-I, 3A, E, F and 4A-I). Masson's trichrome staining demonstrated markedly greater collagen deposition in the 'inhibitor' groups compared with the corresponding 'no inhibitor' groups (Fig. 5). Notably, compared with the S group, SMAD2 and SMAD3 expression levels in the Si group were significantly higher, whereas there was no significant increase was observed in the Mi group compared with the M group (Fig. 3A, C and D). In addition, compared with the corresponding 'no inhibitor' groups, the TGF-β1 expression levels in the Mi group were significantly higher, whereas there was no significant increase in the Si group (Fig. 3A, G).

Following TGF-β1 treatment, TGF-β1-stimulated TCMK-1 cells exhibited significantly higher expression levels of α-SMA, collagen-I, FN, SMAD2, SMAD3, pSMAD2 and pSMAD3 in the siRNA-CTSS group compared with the scramble group, with lower E-cadherin levels; in the absence of TGF-β1, such changes did not occur (Figs. 2J-N, 3B, I-L and 4J-N).

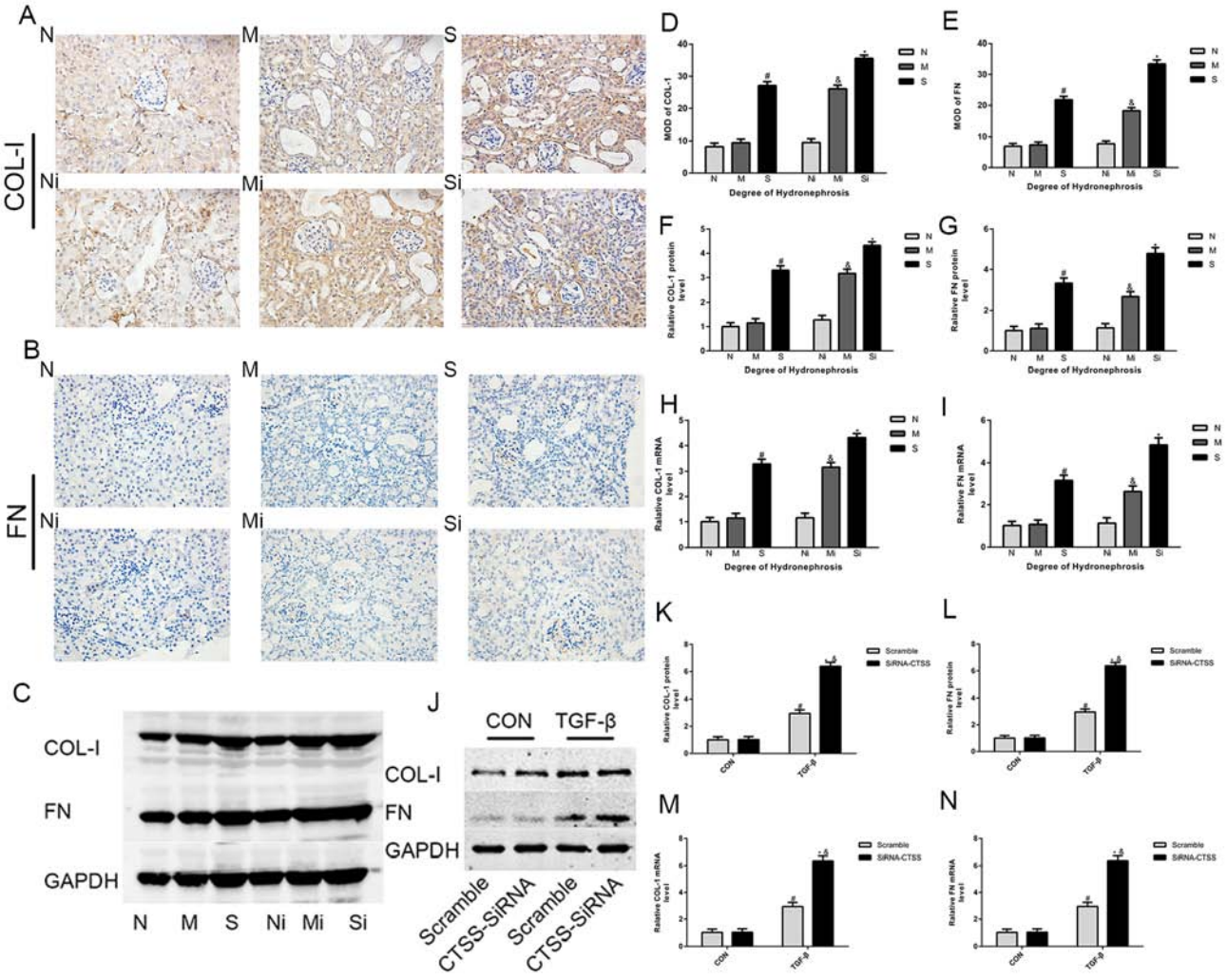

Figure 2. Reducing the expression of CTSS can increase the deposition of ECM. (A, B, D and E) COL-1 and FN measured by immunohistochemistry (magnification, x400) in mice treated with LY3000328 or not; (C, F and G) COL-1 and FN measured by WB in mice treated with LY3000328 or not; (H and I) COL-1 and FN measured by qPCR in mice treated with LY3000328 or not; (J-L) COL-1 and FN measured by WB in TCMK-1 cells treated with TGF-β or not; (M and N) COL-1 and FN measured by qPCR in TCMK-1 cells treated with TGF-β or not. The data are shown as the mean ± standard deviation; $^{\#}$P<0.05 vs. the N group or corresponding control (CON), $^{\&}$P<0.05 vs. the M group or corresponding scramble, *P<0.05 vs. the S group or corresponding control (CON). Grouping: The N groups (N-no inhibitors, Ni-inhibitors), no hydronephrosis; the M groups (M-no inhibitors, Mi-inhibitors), mild hydronephrosis; and the S groups (S-no inhibitors, Si-inhibitors), severe hydronephrosis. CTSS, cathepsin S; ECM, extracellular matrix; WB, western blotting; qPCR, quantitative PCR.

Discussion

Obstructive nephropathy is often accompanied by varying degrees of hydronephrosis (18). Research on the pathogenesis of hydronephrosis may contribute to the development of antifibrotic therapeutic protocols. To the best of our knowledge, the present study was the first to reveal that CTSS may be involved in renal fibrosis and that the downregulation of CTSS may promote ECM deposition and EMT. Furthermore, the regulation of renal fibrosis by CTSS may be related to the phosphorylation of SMAD2 and SMAD3.

The causes of renal fibrosis are diverse; inflammation, injury, ischemia and reperfusion can all lead to renal fibrosis (19-23). There have been multiple studies on the cellular mechanisms of renal fibrosis, many of which primarily focused on EMT and ECM (24,25). Nevertheless, the mechanism of renal fibrosis remains controversial (26-28). The role of EMT in the progression of renal fibrosis has not been determined (29,30). Nevertheless, kidney fibrosis with various causes eventually occurs through the deposition of ECM. CTSS is a member of the cysteine protease family; it degrades certain components of ECM, such as collagen and FN (31). Inhibition of CTSS may directly or indirectly affect the expression or degradation of these ECM proteins.

The expression of CTSS was measured in kidneys with varying degrees of hydronephrosis prior to treatment with the selective CTSS inhibitor LY3000328 (32) to observe whether reducing the expression of CTSS may affect the progression of renal fibrosis. In the 'non-inhibitor' groups, the collagen-I and FN levels in the M group were insignificantly higher compared with the N group, whereas significant ECM deposition was observed in the S group. As important components of ECM, collagen-I and FN are often used to indicate the severity of fibrosis (33). In the non-inhibitor groups, ECM deposition did not change significantly in the M group but increased significantly in the S group. This suggested that although hydronephrosis is associated with renal fibrosis, only hydronephrosis develops to a certain stage leading to

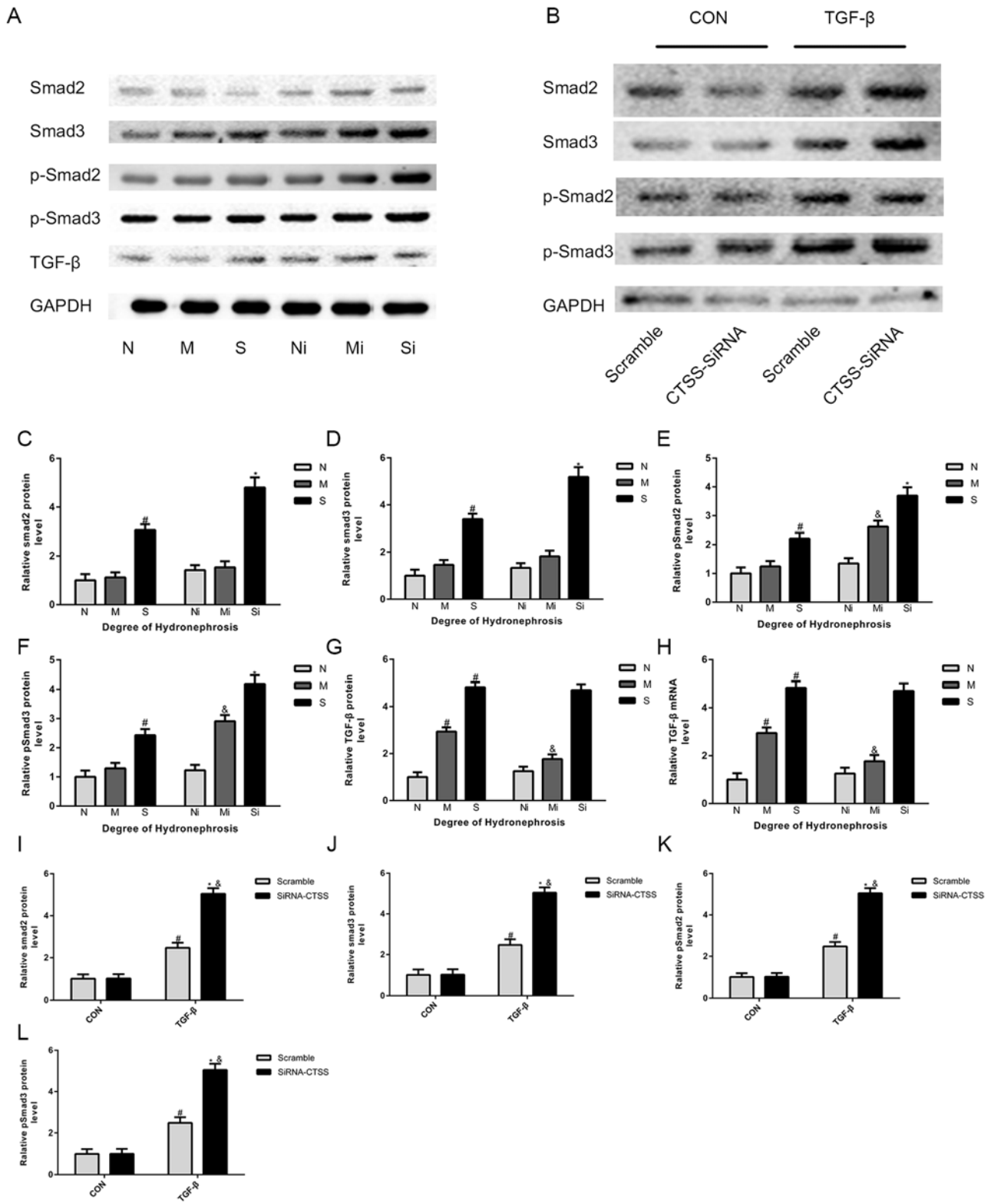

Figure 3. The expression of TGF-β signaling pathway-related factors changes after interference with the expression of CTSS. (A, C-G) Smad2/3, pSmad2/3 and TGF-β measured by WB in mice treated with LY3000328 or not; (B, I-L) Smad2/3, pSmad2/3 and TGF-β measured by WB in TCMK-1 cells treated with TGF-β or not; (H) TGF-β measured by qPCR in mice treated with LY3000328 or not. The data are shown as the mean ± standard deviation; $^{\#}$P<0.05 vs. the N group or corresponding control (CON), $^{\&}$P<0.05 vs. the M group or corresponding scramble, *P<0.05 vs. the S group or corresponding control (CON). Grouping: The N groups (N-no inhibitors, Ni-inhibitors), no hydronephrosis; the M groups (M-no inhibitors, Mi-inhibitors), mild hydronephrosis; and the S groups (S-no inhibitors, Si-inhibitors), severe hydronephrosis. TGF, transforming growth factor; CTSS, cathepsin S; WB, western blotting; qPCR, quantitative PCR.

observable renal fibrosis. Although previous CTSS-related studies have primarily focused on its role in the degradation of ECM, a study by LeBleu *et al* (34) also questioned the importance of EMT in renal fibrosis progression, suggesting

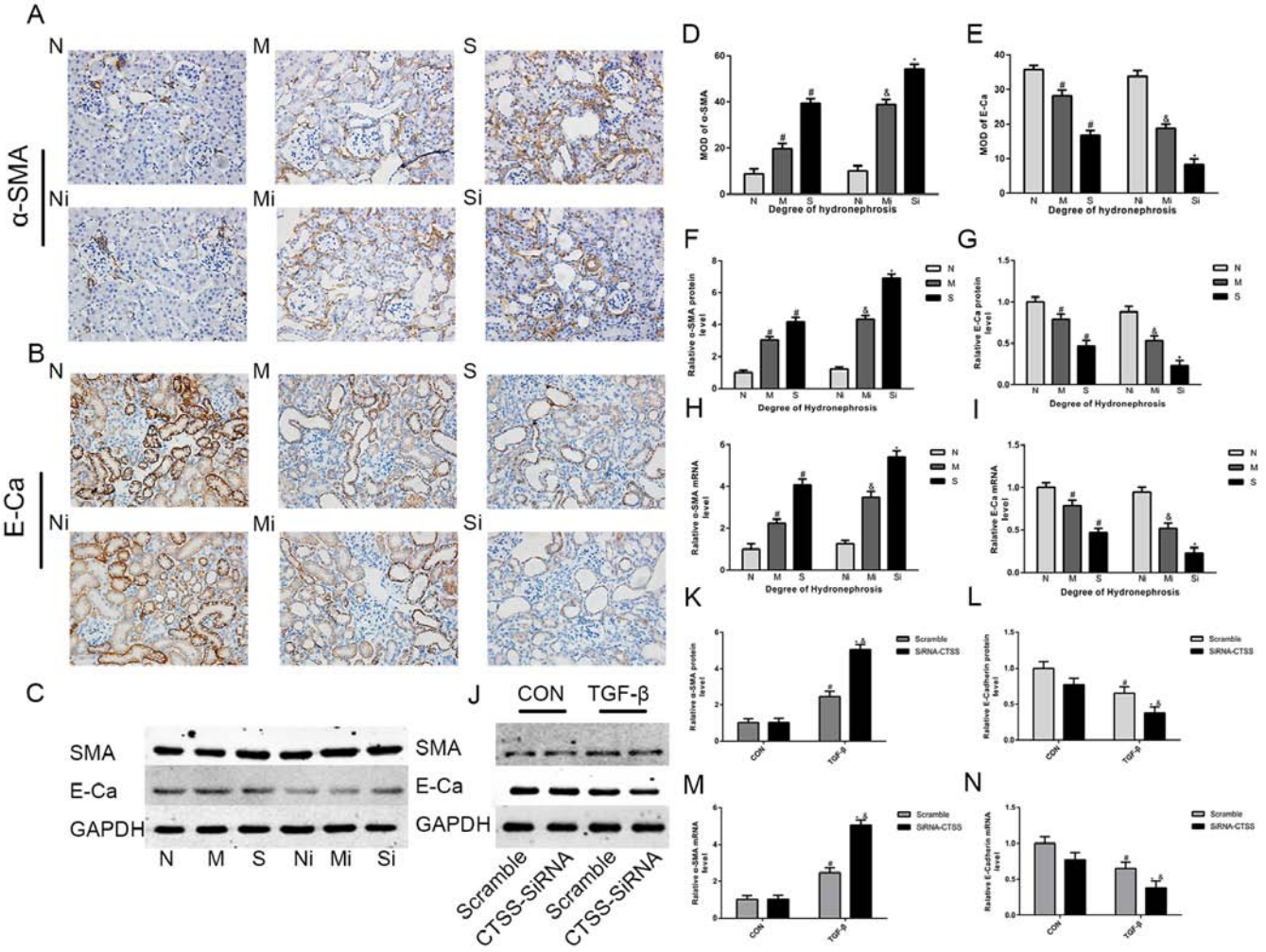

Figure 4. Reducing the expression of CTSS can exacerbate EMT. (A, B, D and E) α-SMA and E-cadherin measured by immunohistochemistry (magnification, x400) in mice treated with LY3000328 or not; (C, F and G) α-SMA and E-cadherin measured by WB in mice treated with LY3000328 or not; (H and I) α-SMA and E-cadherin measured by qPCR in mice treated with LY3000328 or not; (J-L) α-SMA and E-cadherin measured by WB in TCMK-1 cells treated with TGF-β or not; (M and N) α-SMA and E-cadherin measured by qPCR in TCMK-1 cells treated with TGF-β or not. The data are shown as the mean ± standard deviation; $^{\#}$P<0.05 vs. the N group or corresponding control (CON), $^{\&}$P<0.05 vs. the M group or corresponding scramble, *P<0.05 vs. the S group or corresponding control (CON). Grouping: The N groups (N-no inhibitors, Ni-inhibitors), no hydronephrosis; the M groups (M-no inhibitors, Mi-inhibitors), mild hydronephrosis; and the S groups (S-no inhibitors, Si-inhibitors), severe hydronephrosis. CTSS, cathepsin S; EMT, epithelial-mesenchymal transition; WB, western blotting; qPCR, quantitative PCR; TGF, transforming growth factor.

that only 5% of the myofibroblasts in the fibrosis process are related to EMT, and that EMT plays only a limited role in the process of fibrosis. In the present study, the expression levels of α-SMA increased in the M and S groups, whereas E-cadherin levels decreased. In the traditional view, EMT is initiated by the activation of α-SMA-positive cells, and increased expression of α-SMA indicates that the cells gradually lose the epithelial phenotype and convert to mesenchymal cells (35). As an epithelial marker, E-cadherin is often used together with α-SMA to monitor the progression of EMT (36). Although the results of the present study cannot confirm whether the complete EMT process was involved in the development of renal fibrosis, a proposal of partial EMT was previously validated by changes in α-SMA and E-cadherin (37). It is uncertain whether epithelial cells eventually transform into mesenchymal cells; epithelial cells may undergo some changes and participate in cell signal transduction during fibrosis. As a classical signaling pathway, the TGF-β1 signaling pathway has been mentioned in several studies (38). In the present study, the expression levels of SMAD2/3 and p-SMAD2/3 were significantly higher in the S group compared with the N group, whereas the levels of TGF-β1 were notably higher in the M group compared with the N group. This result suggested that fibrosis of the hydronephrotic kidney may involve activation of the TGF-β1 signaling pathway.

As SMAD2/3 is a downstream cytokine of TGF-β1, the changes in TGF-β1 are consistent with SMAD2/3 and p-SMAD2/3 in a number of studies (39,40). Cathepsin B has been reported to affect the activation of TGF-β1, and CTSS has been proposed to regulate the activation of TGF-β1 (41,42). Compared with group M, the expression of TGF-β in Mi group increased significantly, while the expression of Smad2 and smad3 did not change significantly. The exception of the Mi group indicates that, in addition to directly affecting phosphorylation of SMAD2/3, the downregulation of CTSS may also have an indirect effect on SMAD2/3 by modulating the expression or activation of TGF-β1 (9,43).

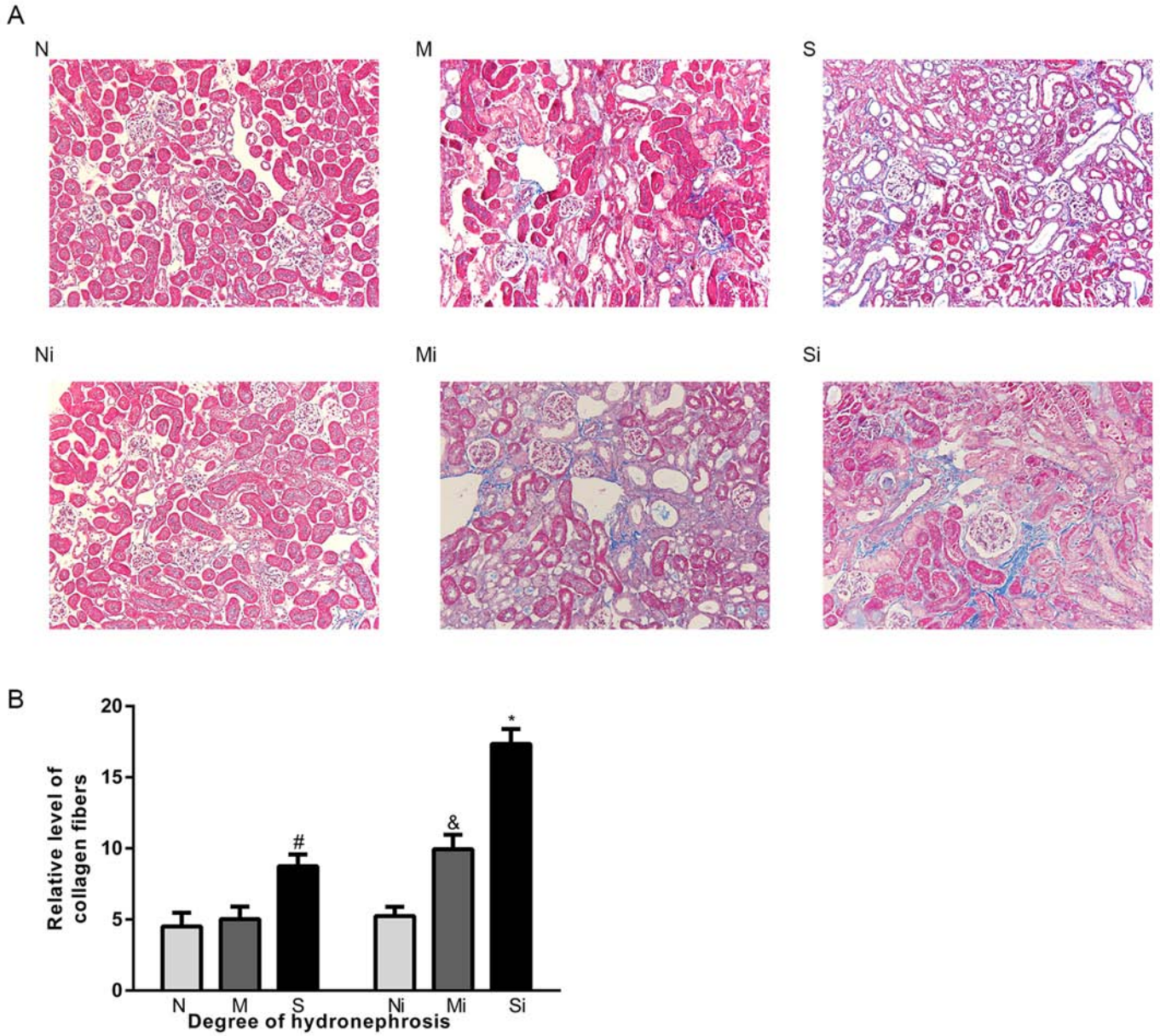

Figure 5. Interfering with the expression of CTSS aggravates renal fibrosis. (A) Masson staining (magnification, x200); (B) Quantitative analysis of the degree of fibrosis. The blue area represents the deposition of collagen. The data are shown as the mean ± standard deviation; $^{\#}$P<0.05 vs. the N group, $^{\&}$P<0.05 vs. the M group, *P<0.05 vs. the S group. Grouping: The N groups (N-no inhibitors, Ni-inhibitors), no hydronephrosis; the M groups (M-no inhibitors, Mi-inhibitors), mild hydronephrosis; and the S groups (S-no inhibitors, Si-inhibitors), severe hydronephrosis. CTSS, cathepsin S.

In the *in vitro* experiments, TGF-β1 was used to stimulate TCMK-1 tubular epithelial cells to construct a cell fibrosis model. Following TGF-β1 stimulation, increased CTSS expression was accompanied by ECM deposition and increased EMT. The opposite changes occurred after siRNA-CTSS treatment. These results indicate that CTSS can affect fibrosis from both EMT and ECM *in vitro*. Inhibition of CTSS expression aggravates fibrosis and this is consistent with the conclusion of the *in vivo* experiment.

In conclusion, the present study demonstrated that CTSS serves an important role in the fibrotic process of hydronephrosis. CTSS may not only mediate the degradation of ECM, but also participate in the regulation of EMT and the TGF-β1 signaling pathway. Therefore, CTSS may serve an important role in antifibrosis treatment.

Acknowledgements

The authors would like to thank the Central Laboratory of Renmin Hospital of Wuhan University for providing relevant experimental facilities and technical support.

Funding

The present study was supported by the National Natural Science Foundation of China (grant no. 81870471).

Availability of data and materials

The datasets used and/or analyzed during the present study are available from the corresponding author on reasonable request.

Authors' contributions

XY, FC and WY designed the study. XY, TR, SZ and XZ performed the experiments. TR, WL, SZ, XZ and JN collected the experimental data. XY and SZ analyzed the experimental data. XY drafted the manuscript. FC, WY and TR revised the paper for intellectual content. All authors read and approved the final manuscript.

Ethics approval and patient consent to participate

The experimental protocol was performed in accordance with the principles and guidelines of the Guide for the Care and Use of Laboratory Animals of the National Institutes of Health. The present study was approved by the Ethics Committee of Renmin Hospital of Wuhan University.

Patient consent for publication

Not applicable.

Competing interests

The authors declare that they have no competing interests.

References

1. Campanholle G, Ligresti G, Gharib SA and Duffield JS: Cellular mechanisms of tissue fibrosis. 3. Novel mechanisms of kidney fibrosis. Am J Physiol Cell Physiol 304: C591-C603, 2013.
2. Liu Y: Cellular and molecular mechanisms of renal fibrosis. Nat Rev Nephrol 7: 684-696, 2011.
3. Lovisa S, Zeisberg M and Kalluri R: Partial Epithelial-to-Mesenchymal transition and other new mechanisms of kidney fibrosis. Trends Endocrinol Metab 27: 681-695, 2016.
4. Nogueira A, Pires MJ and Oliveira PA: Pathophysiological mechanisms of renal fibrosis: A review of animal models and therapeutic strategies. In Vivo 31: 1-22, 2017.
5. Pogorzelska A, Żołnowska B and Bartoszewski R: Cysteine cathepsins as a prospective target for anticancer therapies-current progress and prospects. Biochimie 151: 85-106, 2018.
6. Akkari L, Gocheva V, Quick ML, Kester JC, Spencer AK, Garfall AL, Bowman RL and Joyce JA: Combined deletion of cathepsin protease family members reveals compensatory mechanisms in cancer. Genes Dev 30: 220-232, 2016.
7. Brix K, Dunkhorst A, Mayer K and Jordans S: Cysteine cathepsins: Cellular roadmap to different functions. Biochimie 90: 194-207, 2008.
8. de Mingo Á, de Gregorio E, Moles A, Tarrats N, Tutusaus A, Colell A, Fernandez-Checa JC, Morales A and Marí M: Cysteine cathepsins control hepatic NF-κB-dependent inflammation via sirtuin-1 regulation. Cell Death Dis 7: e2464, 2016.
9. Chen H, Wang J, Xiang M, Lin Y, He A, Jin C, Guan J, Sukhova GK, Libby P, Wang JA and Shi GP: Cathepsin S-mediated fibroblast trans-differentiation contributes to left ventricular remodelling after myocardial infarction. Cardiovasc Res 100: 84-94, 2013.
10. Cerne D, Stern I, Marc J, Cerne A, Zorman D, Krzisnik-Zorman S and Kranjec I: CTSS activation coexists with CD40 activation in human atheroma: Evidence from plasma mRNA analysis. Clin Biochem 44: 438-440, 2011.
11. Weldon S, McNally P, McAuley DF, Oglesby IK, Wohlford-Lenane CL, Bartlett JA, Scott CJ, McElvaney NG, Greene CM, McCray PB Jr and Taggart CC: miR-31 dysregulation in cystic fibrosis airways contributes to increased pulmonary Cathepsin S production. Am J Respir Crit Care Med 190: 165-174, 2014.
12. Hamm-Alvarez SF, Janga SR, Edman MC, Madrigal S, Shah M, Frousiakis SE, Renduchintala K, Zhu J, Bricel S, Silka K, *et al*: Tear Cathepsin S as a candidate biomarker for Sjögren's syndrome. Arthritis Rheumatol 66: 1872-1881, 2014.
13. Cao Z, Yu W, Li W, Cheng F, Xia Y, Rao T, Yao X, Zhang X and Larré S: Acute kidney injuries induced by various irrigation pressures in rat models of mild and severe hydronephrosis. Urology 82: 1453.e9-e16, 2013.
14. Cao Z, Yu W, Li W, Cheng F, Rao T, Yao X, Zhang X and Larré S: Oxidative damage and mitochondrial injuries are induced by various irrigation pressures in rabbit models of mild and severe hydronephrosis. PLoS One 10: e127143, 2015.
15. Seseke F, Thelen P and Ringert RH: Characterization of an animal model of spontaneous congenital unilateral obstructive uropathy by cDNA microarray analysis. Eur Urol 45: 374-381, 2004.
16. Vielhauer V, Anders HJ, Mack M, Cihak J, Strutz F, Stangassinger M, Luckow B, Gröne HJ and Schlöndorff D: Obstructive nephropathy in the mouse: Progressive fibrosis correlates with tubulointerstitial chemokine expression and accumulation of CC chemokine receptor 2- and 5-positive leukocytes. J Am Soc Nephrol 12: 1173-1187, 2001.
17. Livak KJ and Schmittgen TD: Analysis of relative gene expression data using real-time quantitative PCR and the 2(-Delta Delta C(T)) method. Methods 25: 402-408, 2001.
18. Inci MF, Ozkan F, Bozkurt S, Sucakli MH, Altunoluk B and Okumus M: Correlation of volume, position of stone, and hydronephrosis with microhematuria in patients with solitary urolithiasis. Med Sci Monitor 19: 295-299, 2013.
19. Kaissling B, Lehir M and Kriz W: Renal epithelial injury and fibrosis. Biochim Biophys Acta 1832: 931-939, 2013.
20. Hongtao C, Youling F, Fang H, Huihua P, Jiying Z and Jun Z: Curcumin alleviates ischemia reperfusion-induced late kidney fibrosis through the APPL1/Akt signaling pathway. J Cell Physiol 233: 8588-8596, 2018.
21. Jha V, Garcia-Garcia G, Iseki K, Li Z, Naicker S, Plattner B, Saran R, Wang AY and Yang C: Chronic kidney disease: Global dimension and perspectives. Lancet 382: 260-272, 2013.
22. Singh SP, Tao S, Fields TA, Webb S, Harris RC and Rao R: Glycogen synthase kinase-3 inhibition attenuates fibroblast activation and development of fibrosis following renal ischemia-reperfusion in mice. Dis Model Mech 8: 931-940, 2015.
23. Meng X, Nikolic-Paterson DJ and Lan HY: Inflammatory processes in renal fibrosis. Nat Rev Nephrol 10: 493-503, 2014.
24. Cho HS, Kim JH, Jang HN, Lee TW, Jung MH, Kim TH, Chang S and Park DJ: Alpha-lipoic acid ameliorates the epithelial mesenchymal transition induced by unilateral ureteral obstruction in mice. Sci Rep 7: 46065, 2017.
25. Bai Y, Lu H, Wu C, Liang Y, Wang S, Lin C, Chen B and Xia P: Resveratrol inhibits epithelial-mesenchymal transition and renal fibrosis by antagonizing the hedgehog signaling pathway. Biochem Pharmacol 92: 484-493, 2014.
26. Li L, Zepeda-Orozco D, Black R and Lin F: Autophagy is a component of epithelial cell fate in obstructive uropathy. Am J Pathol 176: 1767-1778, 2010.
27. Humphreys BD, Lin SL, Kobayashi A, Hudson TE, Nowlin BT, Bonventre JV, Valerius MT, McMahon AP and Duffield JS: Fate tracing reveals the pericyte and not epithelial origin of myofibroblasts in kidney fibrosis. Am J Pathol 176: 85-97, 2010.
28. Iwano M, Plieth D, Danoff TM, Xue C, Okada H and Neilson EG: Evidence that fibroblasts derive from epithelium during tissue fibrosis. J Clin Invest 110: 341-350, 2002.
29. Kriz W, Kaissling B and Le Hir M: Epithelial-mesenchymal transition (EMT) in kidney fibrosis: Fact or fantasy? J Clin Invest 121: 468-474, 2011.
30. Fragiadaki M and Mason RM: Epithelial-mesenchymal transition in renal fibrosis-evidence for and against. Int J Exp Pathol 92: 143-150, 2011.
31. Kryczka J and Boncela J: Proteases revisited: Roles and therapeutic implications in fibrosis. Mediators Inflamm 2017: 2570154, 2017.
32. Jadhav PK, Schiffler MA, Gavardinas K, Kim EJ, Matthews DP, Staszak MA, Coffey DS, Shaw BW, Cassidy KC, Brier RA, *et al*: Discovery of Cathepsin S inhibitor LY3000328 for the treatment of abdominal aortic aneurysm. ACS Med Chem Lett 5: 1138-1142, 2014.
33. Cutolo M, Ruaro B, Montagna P, Brizzolara R, Stratta E, Trombetta AC, Scabini S, Tavilla PP, Parodi A, Corallo C, *et al*: Effects of selexipag and its active metabolite in contrasting the profibrotic myofibroblast activity in cultured scleroderma skin fibroblasts. Arthritis Res Ther 20: 77, 2018.
34. LeBleu VS, Taduri G, O'Connell J, Teng Y, Cooke VG, Woda C, Sugimoto H and Kalluri R: Origin and function of myofibroblasts in kidney fibrosis. Nat Med 19: 1047-1053, 2013.

35. O'Connor JW, Mistry K, Detweiler D, Wang C and Gomez EW: Cell-cell contact and matrix adhesion promote αSMA expression during TGFβ1-induced epithelial-myofibroblast transition via Notch and MRTF-A. Sci Rep 6: 26226, 2016.
36. Louis K and Hertig A: How tubular epithelial cells dictate the rate of renal fibrogenesis? World J Nephrol 4: 367-373, 2015.
37. Grande MT, Sánchez-Laorden B, López-Blau C, De Frutos CA, Boutet A, Arévalo M, Rowe RG, Weiss SJ, López-Novoa JM and Nieto MA: Snail1-induced partial epithelial-to-mesenchymal transition drives renal fibrosis in mice and can be targeted to reverse established disease. Nat Med 21: 989-997, 2015.
38. Muñoz-Félix JM, González-Núñez M, Martínez-Salgado C and López-Novoa JM: TGF-β/BMP proteins as therapeutic targets in renal fibrosis. Where have we arrived after 25 years of trials and tribulations? Pharmacol Ther 156: 44-58, 2015.
39. Zhang D, Sun L, Xian W, Liu F, Ling G, Xiao L, Liu Y, Peng Y, Haruna Y and Kanwar YS*:* Low-dose paclitaxel ameliorates renal fibrosis in rat UUO model by inhibition of TGF-beta/Smad activity. Lab Invest 90: 436-447, 2010.
40. Cheng X, Gao W, Dang Y, Liu X, Li Y, Peng X and Ye X: Both ERK/MAPK and TGF-Beta/Smad signaling pathways play a role in the kidney fibrosis of diabetic mice accelerated by blood glucose fluctuation. J Diabetes Res 2013: 463740, 2013.
41. Moles A, Tarrats N, Fernández-Checa JC and Marí M: Cathepsin B overexpression due to acid sphingomyelinase ablation promotes liver fibrosis in niemann-pick disease. J Biol Chem 287: 1178-1188, 2012.
42. Moles A, Tarrats N, Fernández-Checa JC and Marí M: Cathepsins B and D drive hepatic stellate cell proliferation and promote their fibrogenic potential. Hepatology 49: 1297-1307, 2009.
43. Somanna A, Mundodi V and Gedamu L: Functional Analysis of cathepsin B-like cysteine proteases from leishmania donovani complex. Evidence for the activation of latent transforming growth factor beta. J Biol Chem 277: 25305-25312, 2002.